

INFLUENCE OF THE ENSO PHENOMENON ON PRECIPITATION IN THE NORTH-WESTERN PART OF MADAGASCAR

RANDRIANARIVELO Eddy Flocaudel¹, HANTA Tina Olga², JAKELY Vertu³,
RANDRIANANDRASANARIVO Raphaëlon Jacques⁴, JOHANESA Fernand⁵, HARY Jean⁶,
MAXWELL Djaffard⁷

¹ PhD student, Doctoral School of Life Engineering and Modeling, University of Mahajanga, Madagascar

² PhD student, Doctoral School of Life Engineering and Modeling, University of Mahajanga, Madagascar

³ PhD student, Doctoral School of Life Engineering and Modeling, University of Mahajanga, Madagascar

⁴ PhD student, Doctoral School of Life Engineering and Modeling, University of Mahajanga, Madagascar

⁵ PhD student, Doctoral School of Life Engineering and Modeling, University of Mahajanga, Madagascar

⁶ Lecturer, Higher Institute of Science and Technology of Mahajanga-Faculty of Science, Technology and Environment, University of Mahajanga, Madagascar

⁷ Professor, Higher Institute of Science and Technology of Mahajanga-Faculty of Science, Technology and Environment, University of Mahajanga, Madagascar

ABSTRACT

This article is based on an analysis of precipitation according to ENSO phenomenon. Self-organizing maps, associated with hierarchical ascending classification, are methods for subdividing our study area. The calculation of the standardized precipitation index is applied to our rainfall data. The anomalous accumulation is used to determine the start dates and end dates of the season. The aim is to characterize the spatio-temporal variability of rainfall in the north-western part of Madagascar. Then, detect during which ENSO phases most often occur the precipitation anomalies (state of humidity or drought) and also the length of the longest or shortest season. The study area is located between longitudes 43°E to 48.5°E and latitudes between 12°S to 18°S. It is subdivided into 3 sub-zones. The daily precipitation data used are available on the ECMWF website for a period of 42 years (1979 to 2020). They correspond to the sum of large-scale precipitation and convective precipitation. Our study area is grouped into three different sub-areas. The maximum amount of precipitation during the La Nina phase does not differ significantly from that observed during the El Niño phase. However, the El Niño episode has more influence on annual precipitation in our study region. In subzone 2, extreme humidity occurred during this phase. Furthermore, the amounts of annual precipitation during the El Niño phase are almost greater than those in La Nina years. On the other hand, the neutral phase often evokes a state of precipitation close to normal. In subzones 1 and 3, the length of the season curiously tends to lengthen during the El Niño phase.

Keywords : Precipitation, SPI, Anomalous accumulation, ENSO, Self-Organizing Map

1. INTRODUCTION

The analysis of the relationships between rainfall variability and ENSO (El Niño/Southern Oscillation) phenomena has been the subject of numerous studies in different regions of the planet since the 1980s [1,2]. Being at the origin of large interannual variations in global climate [3,4], the ENSO phenomenon affects the degree of abnormality of

precipitation distribution such as excess precipitation (coasts of Peru and Ecuador) or the precipitation deficit in other regions (Indonesia and South-East Africa) [5]. In Madagascar, in general, annual rains are decreasing, only the western part receives more rains [6]. This work proposes the analysis of the influence of the ENSO phenomenon on precipitation in the North-West part of Madagascar in order to characterize any relationship between this phenomenon and precipitation in this area.

2. METHODOLOGIES

2.1 Study area and database

Our study area is delimited by longitude between 43°E to 48.5°E and latitude 12°S to 18°S. It includes the Boeny, Sofia regions and part of the Diana, Melaky Betsiboka and Alaotra Mangoro regions. The individuals (A1, A2, ..., W25) represent the intersection between longitudes and latitudes. In total, we have 575 points, with a grid of 0.25° x 0.25° (Fig-1).

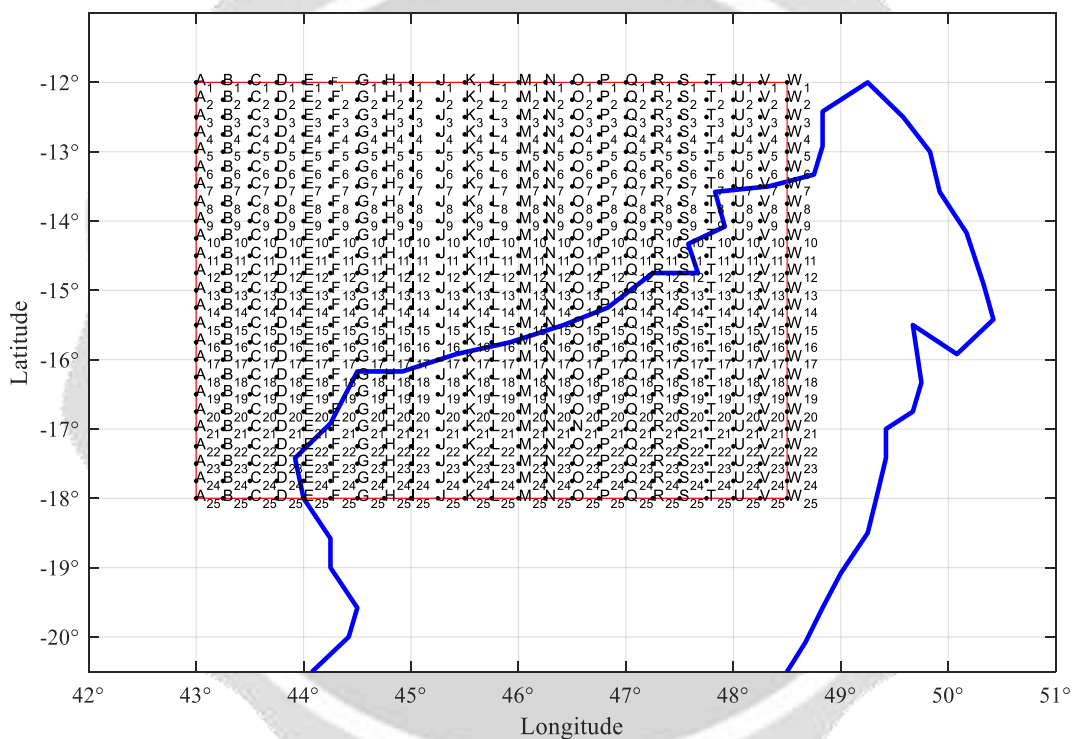


Fig-1: Representation of individuals in the study area

2.2 Data collection

The precipitation data used is that of ERA5 from the fifth generation ECMWF reanalysis for global climate and weather over the last 8 decades (from 1940 to today). This parameter is the accumulated liquid and frozen water, including rain and snow, that falls to the Earth's surface. For ENSO indices, we used three-month moving average data from NOAA ERSST V5 SST Anomalies in Niño 3.4 (5N-5S, 120-170W).

2.3 Self-Organizing Map (SOM)

The “Self-Organizing Map” also called “Kohonen Network” is a very powerful neural method for data classification [7]. The SOM is an unsupervised artificial neural network. The SOM map will be composed of two layers, the first (input layer) represents all the individuals to be classified and the second (topological layer) is composed of neurons

according to the chosen geometry. In the map, each neuron is connected to adjacent neurons, which makes it possible to introduce the notion of distance between neurons or neighborhoods. For the hexagon, the neuron in the middle has 18 neighbors (Fig-2).

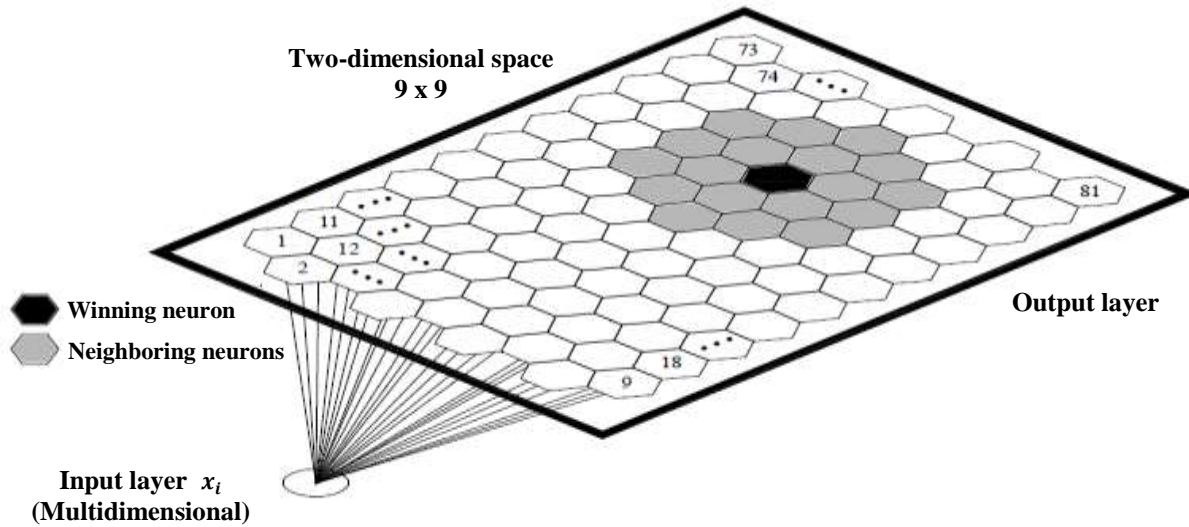


Fig-2 : SOM model structure with a winning neuron and its neighbors [8]

We distinguish two essential steps in the adaptation of the theoretical model [9, 10] :

- Competition phase : the weights of the winning neuron j^* (bmu) as well as those of its topological neighbors are modified so that they are closer to the example presented. This modification is done according to the equation :

$$w_j(t + 1) = w_j(t) + [\varepsilon(t) \cdot h_{j^*} \cdot (X(t) - w_j(t))] \tag{1}$$

where t designates time, $\varepsilon(t)$ is the learning step which decreases with time t and less than 1, h_{j^*} is the neighborhood function of the winning neuron.

With

$$h_j(k, t) = \exp \left[-\frac{d^2(j,k)}{2\sigma^2(t)} \right] \tag{2}$$

$$\sigma(t) = \sigma_i \left(\frac{\sigma_f}{\sigma_i} \right)^{\frac{t}{t_{\max}}} \tag{3}$$

σ_i and σ_f being respectively the initial and final standard deviation, t_{\max} is the total time, $d^2(j, k)$ distance in the neuron map k and j .

- Adaptation phase : We modify the position of the prototypes so as to bring them closer to the individual presented to the network. The prototypes are all the closer to the individual in question the closer they are on the map to the winning neuron. The weighting making it possible to determine the extent of the modifications of position in space is thus a function of the distance on the map between the winning neuron and the neuron considered.

2.4 Standardized Precipitation Index (SPI)

The standardized precipitation index allows us to detect the dryness or humidity of periods in a region. This index is defined by [11, 12] :

$$SPI = \frac{P_i - P_m}{\sigma} \tag{4}$$

2.5 Ascending Hierarchical Classification (AHC)

The Ascending Hierarchical classification will be applied to the output of the Kohonen map, calculation on the Ward method [13].

3. RESULTS

3.1 Self-Organizing Map and Ascending Hierarchical Classification (SOM-AHC)

The output layer is composed of 120 neurons (10 lines × 12 columns). In order to assess the convergence of our algorithm, the figure (Fig-3) shows whether it has stabilized during the iterations or not. Convergence is reached at 3500 iterations (after a strong decrease, we observe a flat shape in the final part of the curve).

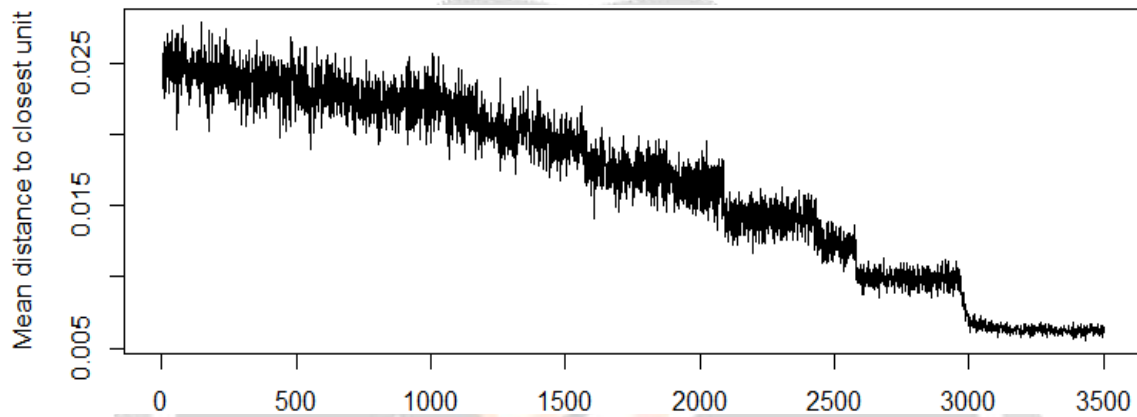


Fig-3 : Training Progress

The figure (Fig-4(a)) displays the number of samples contained in each neuron. This graph reveals that out of 120 neurons, only one (gray color) contains no observations. We can see that the neurons colored white have fewer samples, while the neurons colored blue have more samples assigned, especially neuron number 84. The figure (Fig-4(b)) is often called U-matrix. It allows you to visualize the distance between each node and its neighbors.

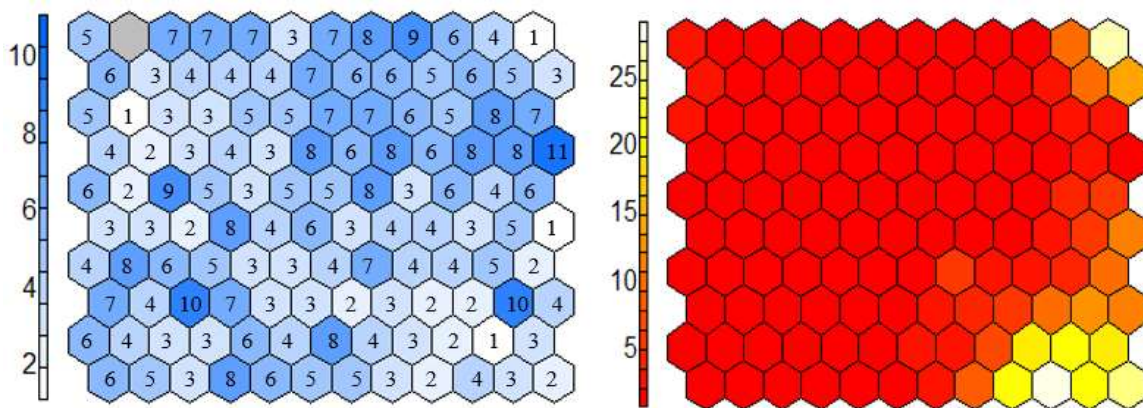


Fig-4 : (a) Number of individuals and (b) distance between neighbors

The distribution of individuals in the map allows us to classify individuals into three sub-zones, which are (Fig-5) :

- subzone 1 (colored green), it brings together the regions of high precipitation throughout the years.
- subzone 2 (colored blue) brings together regions of high precipitation during the dry season.
- subzone 3 (colored in cyan), it brings together the regions where there is little rain during the dry season.

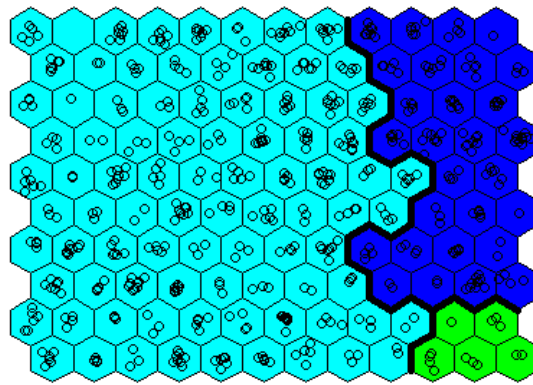


Fig-5 : Distribution of individuals in the SOM map

The climatological averages of precipitation in the three sub-zones are represented by the figure (Fig-6).

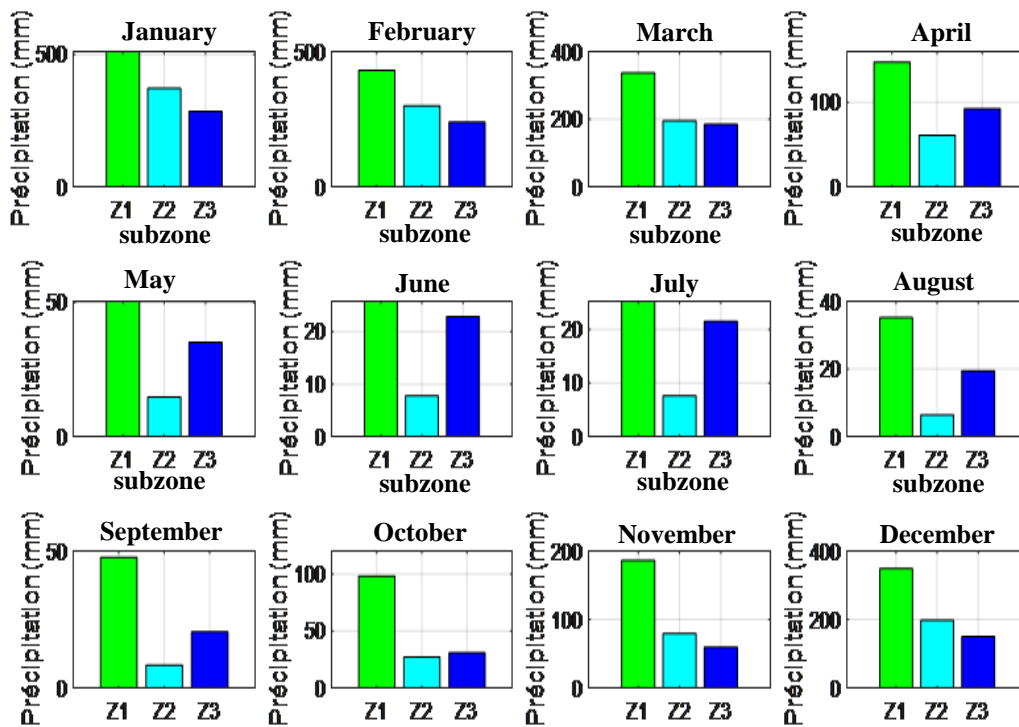


Fig-6 : Climatological average of precipitation in the three sub-zones

The next figures (Fig-7) illustrates the spatial representation of the Kohonen network output in three classes.

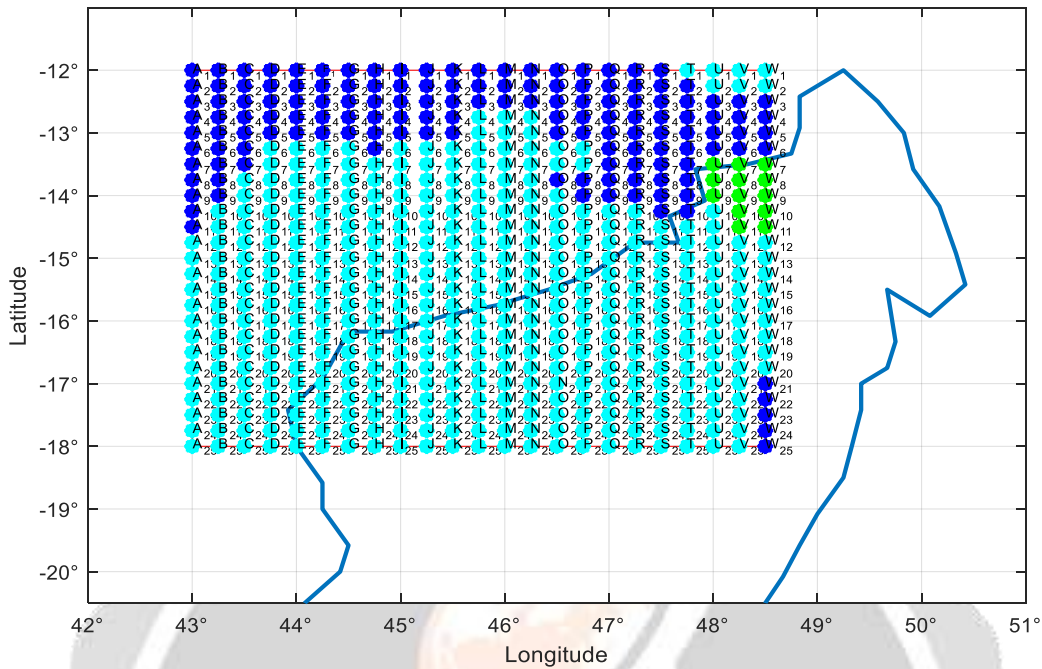
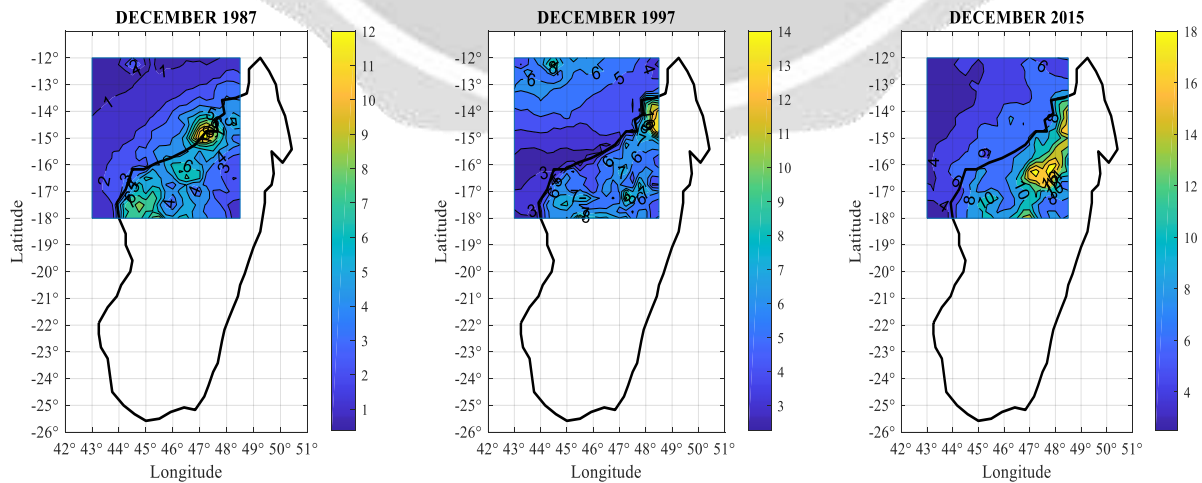


Fig-7 : Zoning of precipitation by the Kohonen network

3.2 Spatial variability of the influences of the ENSO phenomenon on precipitation in the study area

In this section, we will analyze monthly variations in precipitation during three months (December to February) of the austral summer of selected El Niño, La Nina and neutral years (neither El Niño nor La Nina). During El Niño episodes (Fig-8), precipitation dominates the eastern part of the study area, especially in the months of December and February. We see the maximum amount of rain around Analalava district, north of Antonibe, Anjajavy, Bealanana district in Ambanja, which can extend to Mampikony district. But in January, precipitation is dominant along the northwest coasts of Madagascar ranging from Maintirano district to Ambanja district. The rate of precipitation is normal during the El Niño phase, it varies on average between 12 mm to 35 mm. There is a deficit of rain at sea level.



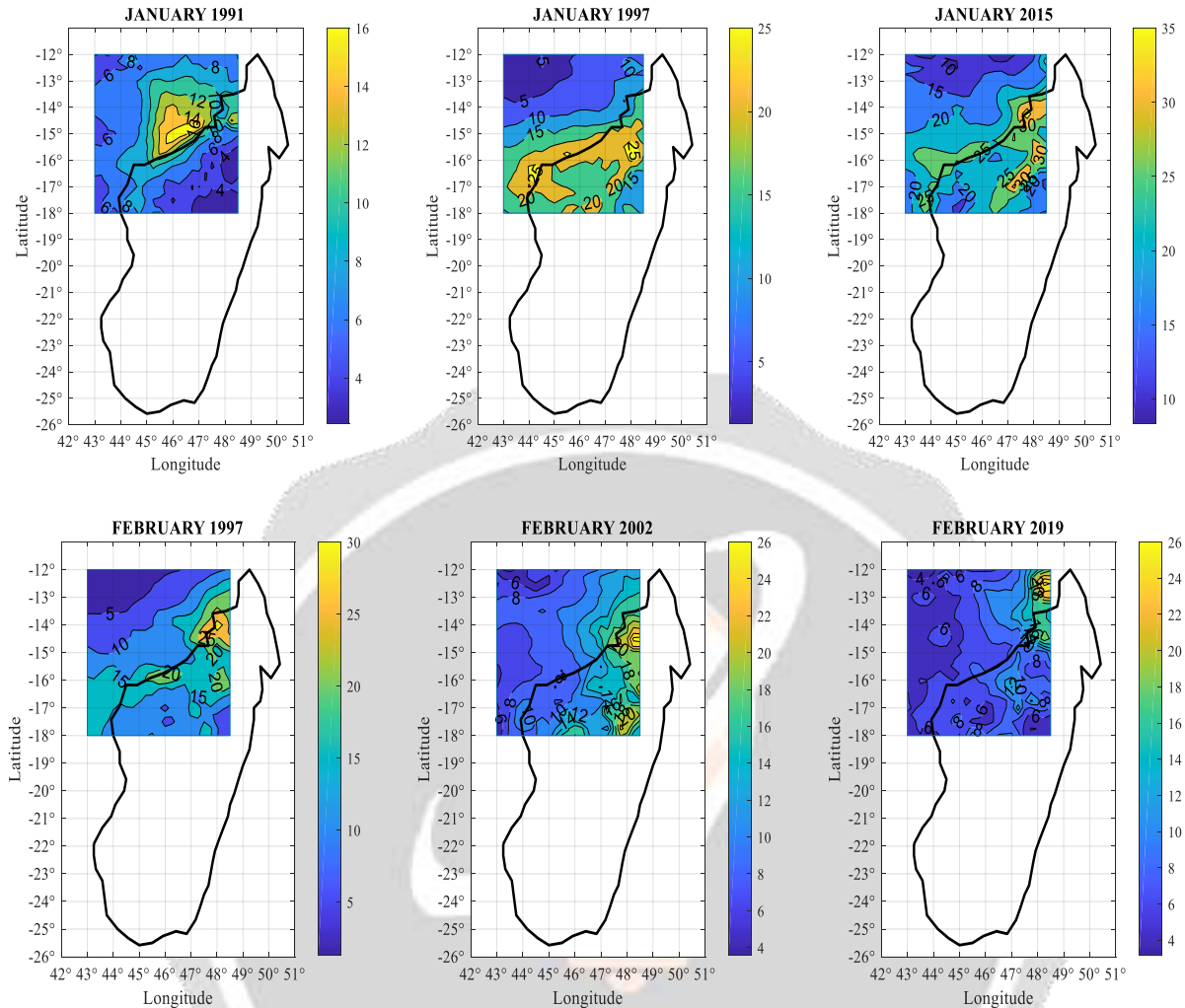
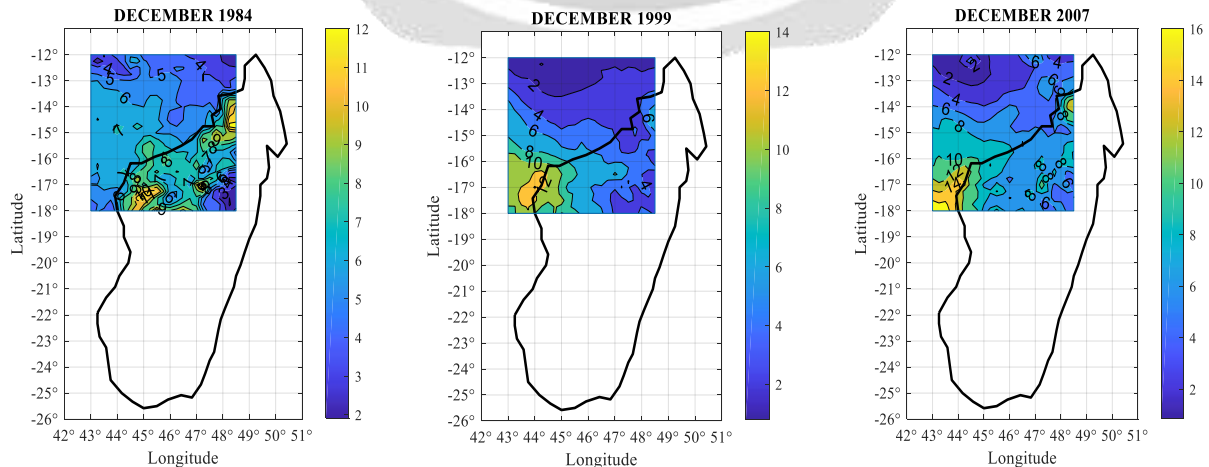


Fig-8 : Monthly variations in precipitation from December to February during the El Niño phase

During the La Nina phase (**Fig-9**), only the northern part of our study area presents a precipitation deficit. We see high rainfall almost throughout the entire part of the north-western region of Madagascar, especially north of Maintirano, in the district of Morafenobe, north of Tsingy de Bemaraha and also in the district of Ambanja and Bealanana. As with the El Niño phase, the maximum precipitation rate varies from 12 mm to 35 mm.



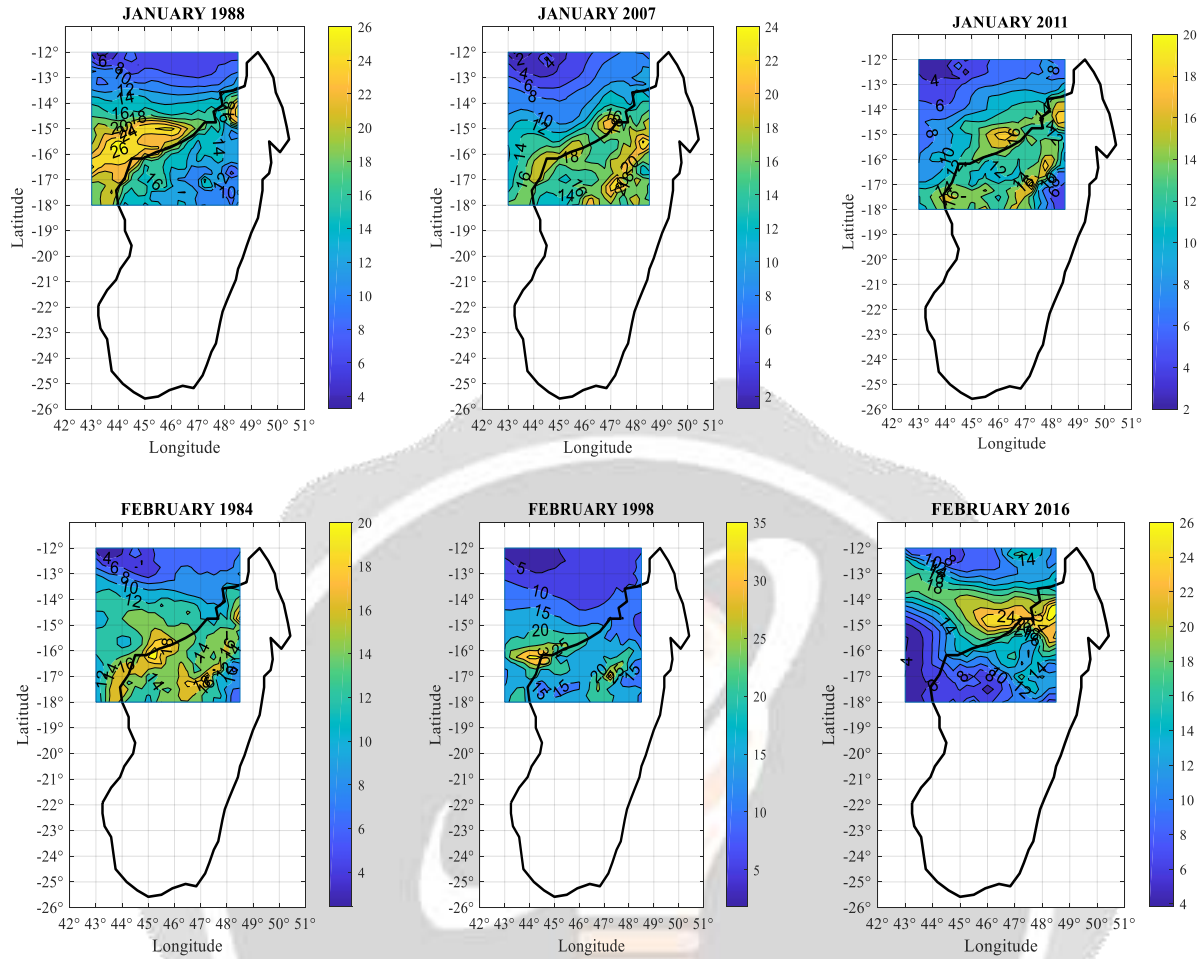
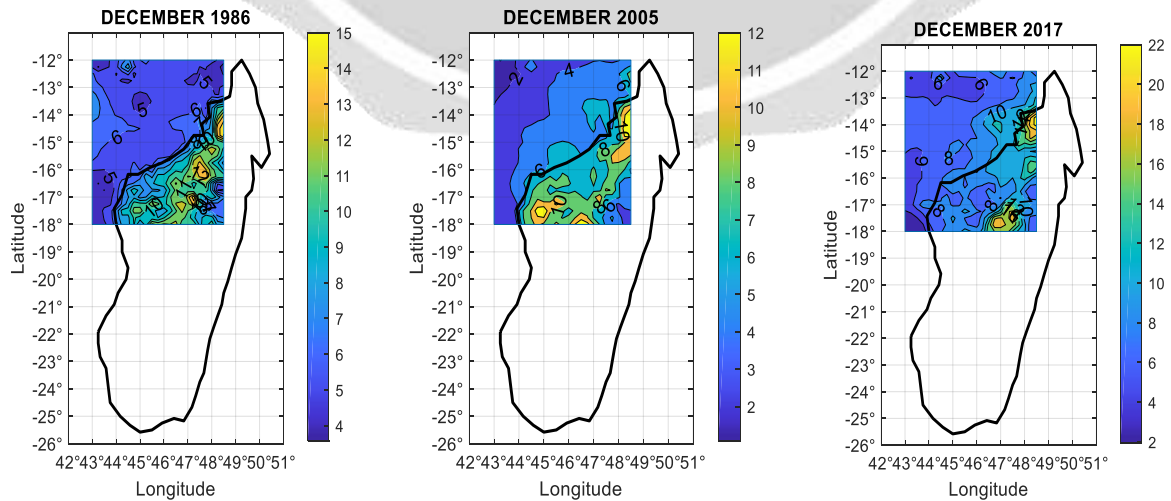


Fig-9 : Monthly variations in precipitation from December to February during the La Nina phase

During the neutral phase (**Fig-10**), precipitation dominates the sea level. In January and February, the precipitation rate reaches 40 mm, which can cause flooding.



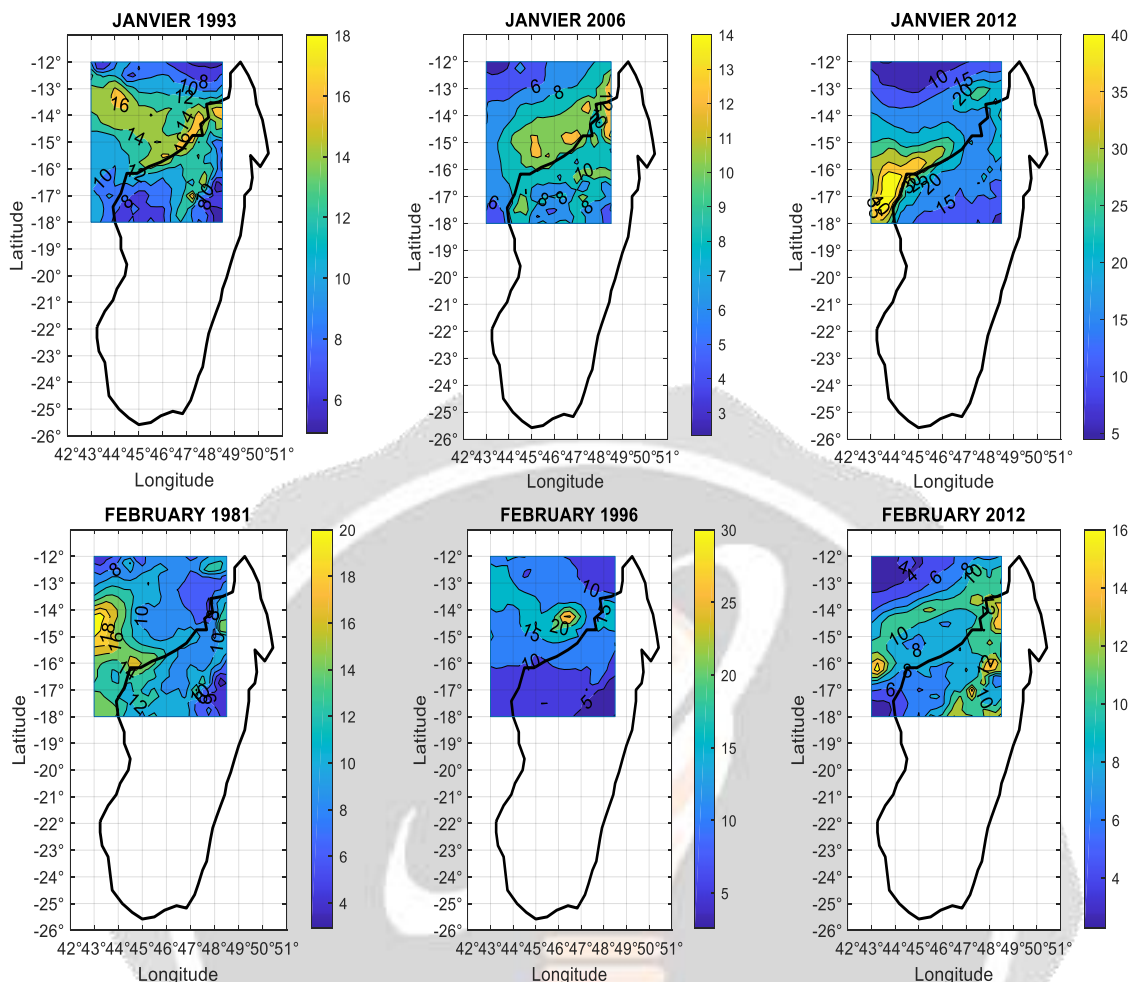


Fig-10 : Monthly variations in precipitation from December to February during the neutral phase

3.3 Standardized precipitation index

The **Chart-1** below represents the standardized precipitation index (SPI) in the three study sub-areas.

In subzone 1, among the four humidities recorded, 50% (one case of extreme humidity and high humidity) of cases appeared during neutral years, 25% during La Niña years and 25% of cases during El Niño phenomenon. We also noticed 50% of drought cases in neutral years, 25% during La Nina years and 25% in El Niño years. Precipitation in this region has no significant difference during the El Niño or La Nina phase.

In subzone 2, the El Niño phase often reveals excess precipitation. Indeed, we noticed 62.5% of cases of humidity including one case of extreme humidity, one case of high humidity and 3 cases of moderate humidity, but the state of dryness only appears once (20% of cases) during this phase. During La Nina episodes, we encountered two cases of humidity (high humidity and moderate humidity) and 40% of cases of drought. The neutral phase is particularly dominated by the normal state of humidity (or dryness).

In subzone 3, the neutral phase evokes the normal state of precipitation. However, one case of high humidity and one case of moderate drought were observed during this phase. In contrast, El Niño phases are often associated with precipitation anomaly. During the passages of this phenomenon, 72.72% (7 out of 11) are linked to deficits or excesses of precipitation (three moderate humidities, one high humidity, three moderate droughts, one severe drought). This allows us to say that there is climate change caused by the increase in the temperature of the surface waters of the Pacific Ocean. As for La Nina episodes, 37.5% cases of humidity and 28.57% cases of drought were recorded.

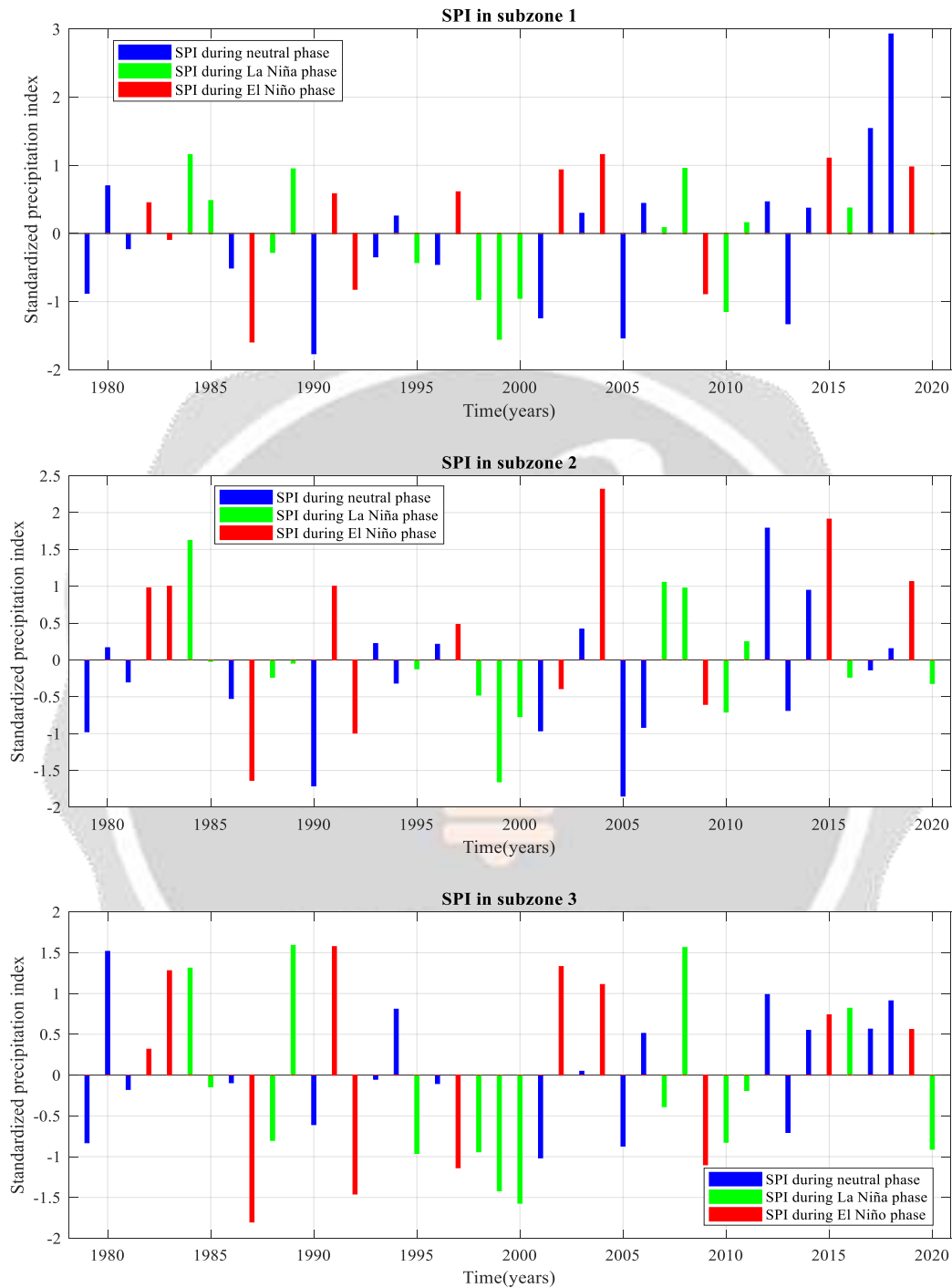


Chart-1 : Standardized Precipitation Index (SPI) in the three study sub-areas

Table-1 illustrates the rainy season parameters in the three sub-zones for 41 seasons. Let's take neutral years as a reference. In subzone 1, during the El Niño phase, the start dates of the rainy season are on average advanced by about 6 days (± 1 day) and the end dates are late by 1 day (± 1 day). The duration of the rainy season increased by approximately 7 days (± 1 day) compared to the neutral phase. For the La Nina phase, the start dates are delayed by 2 days (± 1 day) and those for the end of rain are also delayed by 1 day (± 1 day). The duration of the rainy season is

the same as that of the neutral year. In subzone 2, for La Nina years, the start dates of the rainy season are on average brought forward by around 6 days (± 1 day) and the end dates are delayed by 2 days (± 1 day). On the other hand, the start dates are brought forward by 4 days (± 1 day) during El Niño and the end of rain dates are brought forward by 4 days (± 1 day). As for the duration of the rainy season, it is on average delayed by 5 days (± 1 day) (La Nina phase) but delayed by 1 day (± 1 day) during El Niño years. In subzone 3, during the El Niño phase, the start dates of the rain are brought forward by 3 days (± 1 day) and those of the end are delayed by 3 days (± 1 day). In fact, the length of the season increased by 6 days (± 1 day). For the La Nina phase, the start dates are the same as those of neutral years and the end dates of rain are 5 days late (± 1 day). As for the duration of the rainy season, we notice an increase of 5 days (± 1 day).

Table-1 : Seasonal parameters depending on the ENSO phenomenon

	Start date (days)			End date (days)			Length of rainy season (days)		
Area 1									
	early	late	Avg.	early	late	Avg.	Min	Max	Avg.
El Niño year	16 -Oct	18-Dec	14-Nov	10-Mar	02-May	04-Apr	103	184	141.86
Neutral Year	23-Oct	21-Dec	20-Nov	12-Mar	27-Apr	03-Apr	95	187	134.69
La Niña Year	06-Nov	08-Dec	22-Nov	17-Mar	23-Apr	04-Apr	100	152	134.43
Area 2									
	early	late	Avg.	early	late	Avg.	Min	Max	Avg.
El Niño year	03-Nov	13-Dec	25-Nov	06-Mar	21-Apr	24-Mar	89	170	120
Neutral Year	11-Nov	26-Dec	29-Nov	09-Mar	19-Apr	28-Mar	92	160	119.69
La Niña Year	06-Nov	07-Dec	23-Nov	08-Mar	14-Apr	26-Mar	93	151	124.21
Area 3									
	early	late	Avg.	early	late	Avg.	Min	Max	Avg.
El Niño year	15-Nov	25-Dec	07-Dec	10-Mar	03-May	03-Apr	76	145	118.36
Neutral Year	19-Nov	05-Jan	10-Dec	13-Mar	27-Apr	31-mar	84	137	112.61
La Niña Year	17-Nov	05-Jan	10-Dec	08-Mar	27-Apr	05-Apr	87	152	117.43

The variation of annual precipitation during the two active phases (El Niño, La Nina) is illustrated in the **Chart-2**. In subzones 1 and 3, we see that the rainfall amounts are almost the same during both phases. Precipitation in the El Niño phase has no significant difference from that recorded in La Nina years. On the other hand, in subzone 2, the maximum amount of rain is spotted during El Niño years. Indeed, it should be noted that during El Niño (red bar), the amounts of rain are almost very high compared to La Nina years. Moreover, in 2004, this area was affected by extreme humidity which coincided with the El Niño episode.

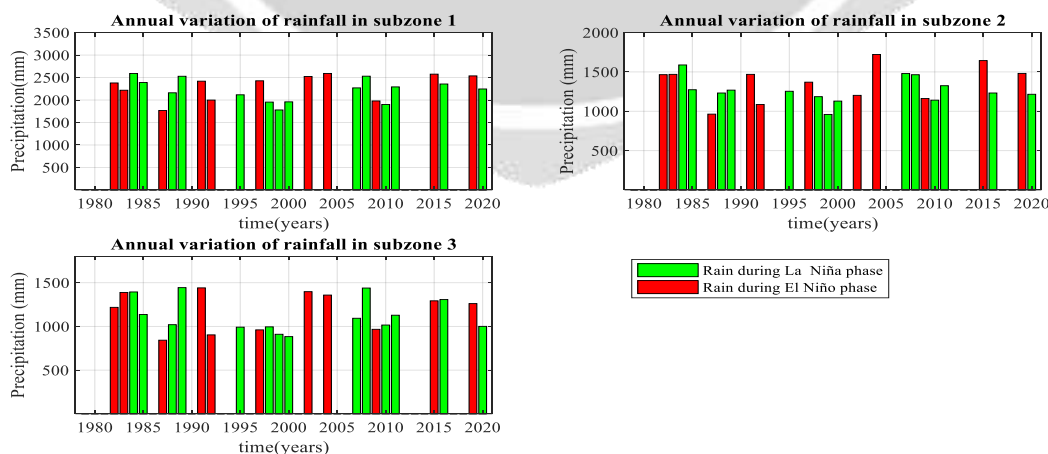


Chart-2 : Annual variations of precipitation in the three study sub-areas depending on El Niño and La Nina phenomena

4. CONCLUSIONS

This study allowed us to analyze the influence of the ENSO phenomenon on rain in the North-West part of Madagascar. The SOM method resulted in a classification of our study area into three different sub-zones (sub-zone with high precipitation all year round, sub-zone with high precipitation during the dry season, sub-zone with low precipitation during the dry season). Even if there does not appear a direct link between the ENSO index and precipitation (weak correlation). A detailed analysis of the spatio-temporal variability of precipitation revealed that the maximum rate of precipitation recorded in the La Nina phase is not different from that of the El Niño phase. We examined the coincidence of the ENSO phenomenon (El Niño, La Nina) between the states of years (wet or dry) and then between the parameters of the seasons. Then we determined the variations in annual precipitation during the active phases of ENSO in the three study sub-areas. Among the seventeen appearances of the neutral phase over the course of 42 years, only one coincides with a state of humidity, with the exception of subzone 1. This phase most often evokes a state of precipitation close to the normal. The El Niño phase has a strong influence on annual precipitation, particularly in subzone 2 ; this phase often evokes precipitation anomaly (an excess or deficit of precipitation). It also affects the longevity of the rainy season in a non-significant way.

5. REFERENCES

- [1]. Rome-Gaspaldy S., Ronchail J., Rainfall in Peru during the ENSO and LNSO phases. Bull The Fr Institute of Andean Studies. 1998;27(3):675-85.
- [2]. Rossel F., Le Goulven P., Cadier E. Spatial distribution of the influence of ENSO on annual precipitation in Ecuador. Rev Sci Water J Water Sci. 1999;12(1):183-200.
- [3]. Soden B., The Sensitivity of the Tropical Hydrological Cycle to ENSO. J Clim - 2000;13:538-49.
- [4]. Gaucherel C., A study of the possible extended influence of the ENSO phenomenon. Geosci Reports. 2004;336(3):175-85.
- [5]. Dewitte O., Update on the phenomena of El Niño, La Niña and the Southern Oscillation. Bulletin of the Geographical Society of Liège, 40, 2001/1, 15-32
- [6]. WWF, https://www.wwf.mg/qui_sommes_nous_2/earth_hour/ (Accessed Nov 18, 2023).
- [7]. T. Kohonen, Self-Organizing Maps, 3rd ed. Berlin: Springer, 2001
- [8]. Farias C., Santos C., Gonçalves Lourenço AM, Carneiro T. Kohonen neural networks for rainfall-runoff modeling: case study of Piancó River Basin. J Urban Environ Eng. 2013;7:176-82.
- [9]. Cottrell M., Letrémy P., Rousset P., Ibbou S., Self-organizing maps for exploratory data analysis and visualization. Journal of the French Statistical Society, French Statistical Society and Mathematics Society of France, 2003, 144 n°4, pp.67-106.
- [10]. V. Lemaire, Self-organizing maps through data analysis (Consulted on Nov 18, 2023).
- [11] GUTTMAN, NB, "Comparing the Palmer drought index and the Standardized Precipitation Index". Journal of the American Water Resources Association, 34(1):113–121. (1998)
- [12] HARY J., "Forecasting drought in the Western Region of Madagascar by different methods", Thesis of the University of Antananarivo, Physics. (2017).
- [13]. Ward JH, Hierarchical Grouping to Optimize an Objective Function. J Am Stat Assoc. March 1963;58(301):236-44.